Critical scattering at the order-disorder phase transition of Si(111)-$\sqrt{3}\times\sqrt{3}R30°$-Au surface: A phase transition with particle exchange

Y. Nakajima
Department of Physics, School of Science, University of Tokyo, 7-3-1 Hongo, Bunkyo-Ku, Tokyo 113, Japan

C. Voges
Institut für Festkörperphysik, Universität Hannover, Appelstraβe 2, D-30167 Hannover, Germany

T. Nagao and S. Hasegawa
Department of Physics, School of Science, University of Tokyo, 7-3-1 Hongo, Bunkyo-Ku, Tokyo 113, Japan

G. Klos and H. Pfnür*
Institut für Festkörperphysik, Universität Hannover, Appelstraβe 2, D-30167 Hannover, Germany
(Received 19 November 1996)

The Si(111)-$\sqrt{3}\times\sqrt{3}$-Au phase, which coexists with three-dimensional islands of excess Au at coverages above 1 monolayer and at temperatures above 700 K, is shown to undergo a temperature driven order-disorder phase transition at 1057 K. The islands act as a reservoir of Au atoms and adjust the chemical potential for the two-dimensional layer during the transition. Due to this particle exchange, the phase transition within the $\sqrt{3}\times\sqrt{3}$R30°-Au has been observed for a chemisorbed layer which is not under the usual constraint of constant coverage, but controlled by the chemical potential. We quantitatively analyzed the critical scattering and experimentally determined its critical exponents β, γ, and ν by high-resolution low-energy electron diffraction. Their values are in good agreement with the expected values of the three-state Potts model, which shows that the transition is continuous without any finite-size effects detectable. [S0163-1829(97)00514-6]

I. INTRODUCTION

Phase transitions and critical phenomena in two dimensions (2D) have attracted wide interest,[1–3] because fluctuations play a much more important role than in 3D so that large deviations from mean-field behavior are observed. From the experimental point of view, investigations of surface superstructures formed by adsorbates and of their continuous phase transitions are very attractive because they give access to basically all universality classes.[4] In particular, order-disorder phase transitions in the three- and four-state Potts universality classes can be and have been successfully studied with adsorbate-induced superstructures.[5,6]

The determination of critical properties of continuous phase transitions in surface systems, is still a challenge to experimentalists. This is because long-range correlations involved close to the critical point of the transition can be easily distorted by all kinds of defects which are mostly due to the substrate surface or the interface. Phase diagrams and, more severely, the critical properties of phase transitions can be strongly changed by the presence of the defects, as shown in several examples both theoretically[7–9] and experimentally.[10–13]

Although critical properties can still be and have successfully been studied on systems with a limited size of unperturbed regions of the surface,[5,6] there is still a high desire for as perfect a sample as possible. One of the most ideal substrates for this purpose seems to be Si(111), which can be easily prepared with extremely low levels of impurities and point defects. Furthermore, various kinds of adsorbate-induced long-range-ordered superstructures with different symmetry, can be prepared on Si(111).

As one of the most popular systems on Si(111), the adsorption of gold on this surface has been extensively studied during the past few decades. A submonolayer of Au induces 5×2 (or 5×1), $\sqrt{3}\times\sqrt{3}$R30°, and 6×6 superstructures,[14] depending on the gold concentration, and its phase diagram is rich and complicated. The $\sqrt{3}\times\sqrt{3}$R30°-Au structure has been studied by total energy calculations[17] and almost all experimental techniques such as low-energy electron diffraction (LEED),[18,19] reflection high-energy electron diffraction (RHEED),[20] transmission electron diffraction,[21,22] ion scattering,[23–27] x-ray diffraction,[28,29] and scanning tunneling microscopy (STM).[30–33] Its local structure within the unit cell varies with temperature and overall Au coverage. Even for the high-temperature $\sqrt{3}$ phase investigated in this study, no generally accepted atomic structural model exists at present. Also the saturation coverage has not yet been determined explicitly, which could be 2/3 monolayer (ML) or 1 ML. In the following, however, we assume it to be 1 ML.

At temperatures above 850 K, where the 5×2 and $\sqrt{3}\times\sqrt{3}$R30° superstructures do not coexist with other phases, they were shown to undergo order-disorder phase transitions around 1070 and 1057 K, respectively. However, their critical properties seemed quite different as revealed by spot-profile analysis in a RHEED experiment.[15,16] For the 5×2 structure, the phase transition seemed to be of first order, while the $\sqrt{3}\times\sqrt{3}$R30° phase showed signs of critical scattering, suggesting a continuous transition. From symmetry considerations, the 5×2 phase should undergo a discontinuous transition, while the $\sqrt{3}\times\sqrt{3}$R30° phase should be-

long to the three-state Potts universality class, if the transition is continuous. However, since the $\sqrt{3}\times\sqrt{3}$R30° unit cell contains more than one Au atoms and the reconstruction is considered to be quite complicated, involving rearrangements of substrate Si atoms, it is not obvious whether predictions of its critical properties from simple symmetry considerations for the unit cell can be applied to this system. An explicit attempt, carried out in this study, to determine the critical exponents of the order-disorder phase transition of the $\sqrt{3}\times\sqrt{3}$R30° layer, will shed light on this question, and will allow conclusions about the disordering process.

In our own studies using STM, it has been clearly shown that the $\sqrt{3}\times\sqrt{3}$R30° phase cannot be obtained in form of large domains at room temperature (RT), but that it is always accompanied by a domain-boundary region that is not apparently well ordered. Nogami *et al.*[30] and Takami *et al.*[32] observed STM images of such a structure, i.e., a well-ordered $\sqrt{3}\times\sqrt{3}$R30° domain (domain A) and a less-ordered domain (domain B). The fractional area of domain B increases with increasing Au coverage, and when the domain A disappears, the 6×6 phase begins to appear. The Au coverage of the $\sqrt{3}\times\sqrt{3}$R30° phase seems to be $\sim$2/3 ML in the domain A. The lack of consensus for the structural model is due in part to the inseparability of these two domains during use of macroscopic-probe techniques.

Although the structure of the $\sqrt{3}\times\sqrt{3}$R30° surface at RT is complicated, it has been revealed recently by Nagao and Hasegawa[34] that the pure $\sqrt{3}\times\sqrt{3}$R30° phase consists of large single domains with well-ordered $\sqrt{3}\times\sqrt{3}$R30° structure at elevated temperatures. It is shown in Fig. 1(a). Please note that this layer contains no domain walls that may act as defects during the phase transition. Thus for the order-disorder phase transition of this superstructure around 1057 K, its low-temperature phase can be considered ideally ordered in long range without being limited by domain boundaries.

Another feature of this system is a Stranski-Krastanov-type structure; when Au coverage exceeds the saturation coverage of the $\sqrt{3}\times\sqrt{3}$R30° phase, the excess Au makes 3D islands that sparcely distribute on the 2D layer. These islands act as reservoirs of Au atoms, so that the chemical potential is completely controlled by temperature during the phase transition in the 2D layer. The Au concentration of the high-temperature phase in the 2D layer is generally different from that of the low-temperature phase ($\sqrt{3}\times\sqrt{3}$R30° structure). Due to exchange of Au atoms between the two-dimensional layer and three-dimensional islands at elevated substrate temperatures, unrenormalized critical exponents should be expected.

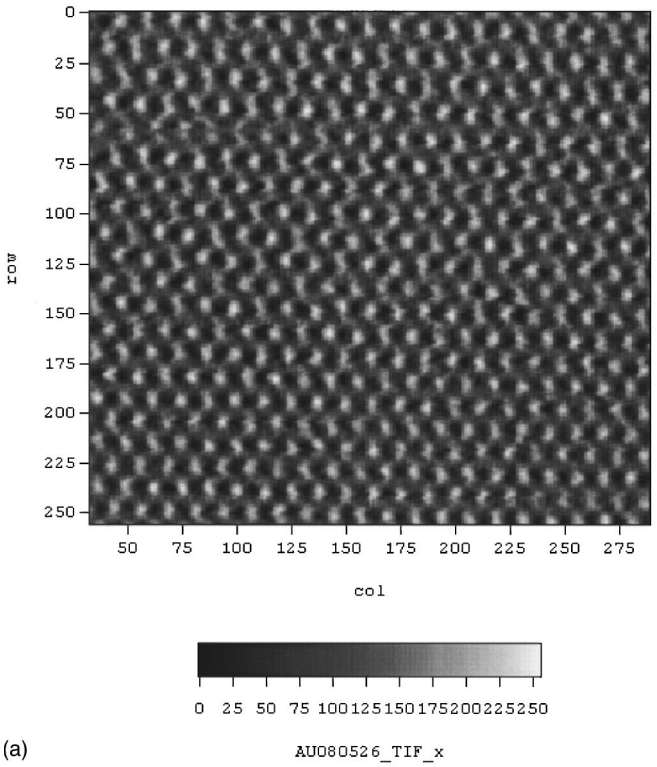

(a)

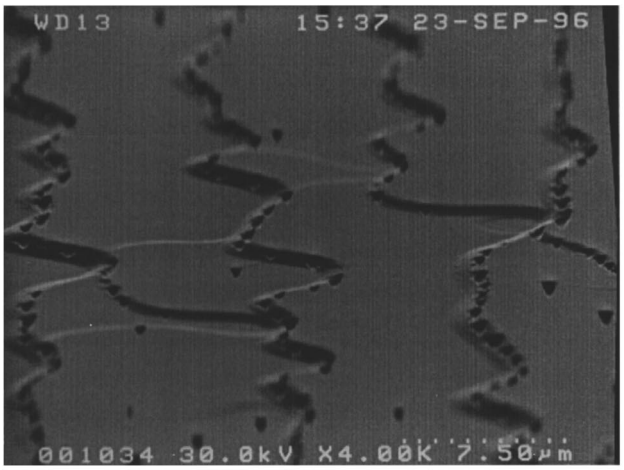

(b)

FIG. 1. (a) Scanning tunneling microscopy image of the $\sqrt{3}\times\sqrt{3}$R30°-Au phase at 800 K. A large single domain can be seen, which is in remarkable contrast to room temperature observations. (b) A grazing-incidence UHV-scanning electron microscopy image after about 2.0-ML-Au deposition onto a clean Si(111) surface at 800 K. Three-dimensional islands composed of excess Au preferentially nucleate at step bunches.

II. EXPERIMENTAL

The apparatus for our measurements has been described in detail recently.[11] In brief, it consists of a UHV system equipped with high-resolution LEED [spot-profile-analyzing LEED, (SPA-LEED)], a cylindrical-mirror analyzer (CMA) and a mass spectrometer, run at a base pressure of 4×10^{-9} Pa. The main analysis was carried out with the SPA-LEED instrument,[35] which had a transfer width larger than 1000 Å.

A Si crystal ($20\times5\times0.4$ mm in size) was cut from highly oriented wafer material with less than 0.1° misorientation off the (111) surface. It was heated resistively with ac current at a frequency of 5 kHz through the sample. In addition, the heating current was modulated with a trapezoid at a frequency of 50 Hz to allow for undisturbed profile measurements of the diffracted electron beams during currentless periods by synchronizing and gating the detector electronics appropriately.

The sample temperature was measured by two W/WRe

thermocouples, which were spot welded to thin tantalum foils. These were crimped around the crystal's rim. The (average) crystal temperature was stabilized by a computerized feedback circuit to better than 0.1 K. Due to our modulation of the heating current, there is also a small temperature modulation with the modulation frequency. Experimentally we determined this modulation to be around 0.2 K at a sample temperature of 1000 K—close to the temperature where the most relevant measurements were carried out—by use of lockin techniques.

A further effect restricted our effective temperature resolution. Due to inhomogeneous contact of the Si sample with the Mo clamps used as sample mounts, a temperature gradient of 0.5 K/mm around 1000 K was observed by the thermocouples and also by IR-pyrometer measurements. Since the area of the crystal surface seen by the electron beam has approximately a diameter of 1 mm, the diffraction intensity is averaged over surface areas which differ in temperature by 0.5 to 1 K. Temperature differences between the location of the thermocouple and the surface area observed by SPA-LEED, on the other hand, are unimportant as long as only reduced temperatures $t=(T-T_c)/T_c$ are of interest, since errors in the absolute temperature influence this quantity very little.

A clean Si surface was prepared by flashing the sample to 1450 K. Care was taken to produce a well-ordered 7×7 structure by slow cooling with 1 K/s, especially in the range 1100–900 K. With this preparation method, effective transfer widths (i.e., including all imperfections on the surface) of 1000 Å were achieved. Au was evaporated from a Au wire onto the clean Si(111) at 900 K. The evaporated amount was controlled by a quartz microbalance. An additional calibration was carried out using the deposition time for completing the 5×2 phase LEED pattern, the coverage of which was determined earlier to be 0.5 ML.[36] The amount of Au evaporated in our case was four times that of the 5×2 phase, i.e., a Au coverage close to 2 ML was used, considerably larger than the saturation of the $\sqrt{3}\times\sqrt{3}$R30° phase. The excess Au atoms are known to form large three-dimensional islands on a two-dimensional $\sqrt{3}\times\sqrt{3}$R30° ordered Au layer, as observed by scanning electron microscopy (SEM) [see Fig. 1(b)]. Due to the high temperature necessary to observe the phase-transition, Au slowly desorbs from the substrate at a rate of $\sim$0.1 ML/h, which was estimated by changes in the LEED pattern to 5×2 close to 1 ML coverage. Since the time necessary to measure one full set of data takes around one hour, the coverage of Au decreases about $\sim$0.1 ML during this time. However, due to the equilibrium with the 3D islands on the surface, just the size of islands decreased and the $\sqrt{3}\times\sqrt{3}$R30° domains did not diminish, as observed by LEED pattern and SEM. In agreement with this finding, the critical temperature of the order-disorder transition of the $\sqrt{3}\times\sqrt{3}$R30° structure was independent of average Au coverage over a very wide range of coverages, as expected by thermal equilibrium with the three-dimensional islands. Only a slow deterioration of the surface quality with an increased amount of defects after weeks of measurements was observed.

The profiles of the $(\frac{1}{3}\frac{1}{3})$ and $(\frac{2}{3}\frac{2}{3})$ superstructure spots were measured and analyzed both in the radial direction with respect to the (00) spot and in the corresponding perpendicular direction. For data analysis, three contributions to the idealized spot profiles $S(\mathbf{q}_\parallel,t)$ were taken into account according to the following parametrization:[37]

$$S(\mathbf{q}_\parallel,t)=I_0(t)\,\delta(\mathbf{q}-\mathbf{q}_0)_\parallel+\frac{\chi_0(t)}{1+(\mathbf{q}-\mathbf{q}_0)_\parallel^2\xi^2(t)}+bg. \qquad (2.1)$$

The first term describes the contribution from *long-range order*. For a continuous phase transition it behaves like $I_0(t)\propto|t|^{2\beta}$ for $T<T_c$, where $\mathbf{q}_\parallel$ is the scattering-vector component parallel to the surface, $t=(T-T_c)/T_c$ is the reduced temperature and $\mathbf{q}_0$ denotes a reciprocal lattice vector of the superstructure. β is the critical exponent of the order parameter Φ ($\Phi\propto\sqrt{I_0}\propto|t|^\beta$). For $T>T_c$, $I_0=0$. The second term describes the contribution of short-range fluctuations of the order parameter (critical scattering). This term is most easily measured above T_c because it is the only remaining term, apart from the background bg, the third term. χ_0 (amplitude of the critical scattering) denotes the susceptibility and ξ the correlation length. For a second-order phase transitions they behave like $\chi_0(t)\propto|t|^{-\gamma}$ and $\xi(t)\propto|t|^{-\nu}$.

The measured profiles always consist of two-dimensional convolutions of an ideal profile [Eq. (2.1)] and the instrumental transfer function (including crystal imperfections). Because of numerical stability, we carried out numerical fits to the experimental profiles instead of trying to deconvolute them. The profile of the superstructure beam observed at a low temperature (T_c-100 K) was used as the instrumental function in the radial direction, whereas in the perpendicular direction it was approximated by a Gaussian of the half width measured in this direction.

III. RESULTS

The $\sqrt{3}\times\sqrt{3}$R30°-Au structure prepared as described above, was found to be perfectly ordered at surface temperatures above 720 K as judged by the measured half widths of its superstructure beams, which were identical to those of the fundamental beams. Below 720 K, a phase transition to the 6×6 superstructure took place, as seen in Fig. 2. The peak intensity of the $(\frac{1}{3}\frac{1}{3})$ spot versus temperature shown there directly reveals the two phase transitions $6\times6\rightarrow\sqrt{3}\times\sqrt{3}$R30° at 720 K and $\sqrt{3}\times\sqrt{3}$R30°$\rightarrow$ disorder at 1057.2 K. The effective Debye-Waller-factor relevant for the second transition was estimated from the slope between 750–850 K, a temperature region which was not influenced by the phase transitions.

The critical temperature of the phase transition $\sqrt{3}\times\sqrt{3}$R30° $\leftrightarrow$ disordered was determined by the inflection point of the Debye-Waller corrected peak-intensity-versus-temperature curve $I(T)$.[38] From the steepness of $I(T)$, and from the precision of the determination of the minimum in dI/dT, an uncertainty in T_c of $\Delta T_c=\pm1.1$ K was estimated (see Fig. 3).

Below T_c, the raw data of the peak intensity of the superstructure beams versus reduced temperature $t=|1-T/T_c|$, corrected by the Debye-Waller factor, were used to determine the critical exponent β of the order parameter by simply fitting the data with a power law. With T_c as determined above, Fig. 4 shows that scaling is found over two orders of magnitude in reduced temperature, $0.002<t<0.1$.

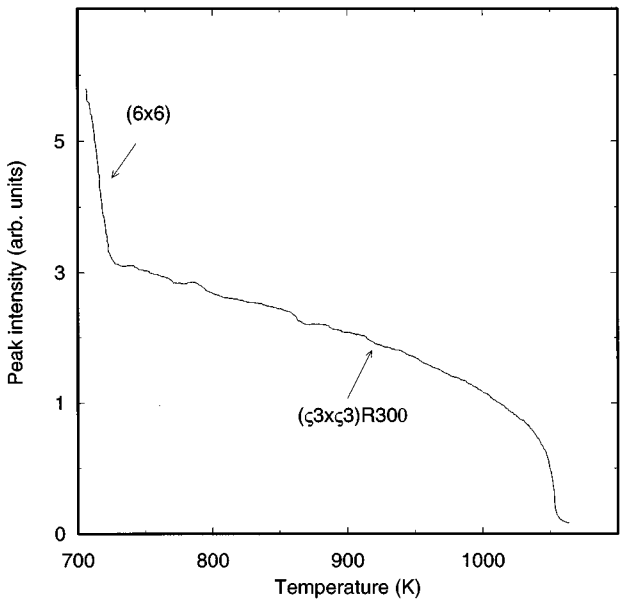

FIG. 2. Peak intensity of a $(\frac{1}{3}\frac{1}{3})$ spot versus temperature (before Debye-Waller correction). The sharp variations in intensity correspond to the phase transitions $6\times6 \rightarrow \sqrt{3}\times\sqrt{3}\mathrm{R}30°$ and $\sqrt{3}\times\sqrt{3}\mathrm{R}30° \rightarrow$ disorder.

The effective critical exponent β of this measurement is 0.109 ± 0.005. The error is mainly caused by the uncertainty in T_c. Below $t<0.002$ the measured peak intensity slightly deviates from the power law. Here either the contribution from critical fluctuations is no longer negligible, or finite-size effects become important. From the analysis of the data above T_c described below, however, the former possibility seems to be more likely. In any case, due to the temperature gradient effect discussed above, measurements much closer to T_c would not be meaningful, so that the available range in reduced temperature would be too small for a quantitative analysis of the critical scattering contribution below T_c. Therefore, no attempt in this direction was made. The same analysis was also tested at the $(\frac{2}{3}\frac{2}{3})$ spot. Within the limits of uncertainty we always obtained the same values for β. The average of the critical exponent β of several runs is given in Table I, which contains four data sets of the $(\frac{1}{3}\frac{1}{3})$ and two of the $(\frac{2}{3}\frac{2}{3})$ spots. The quoted limits of uncertainty contain both the statistical error and the uncertainty in T_c, which contribute about equally to the error limits.

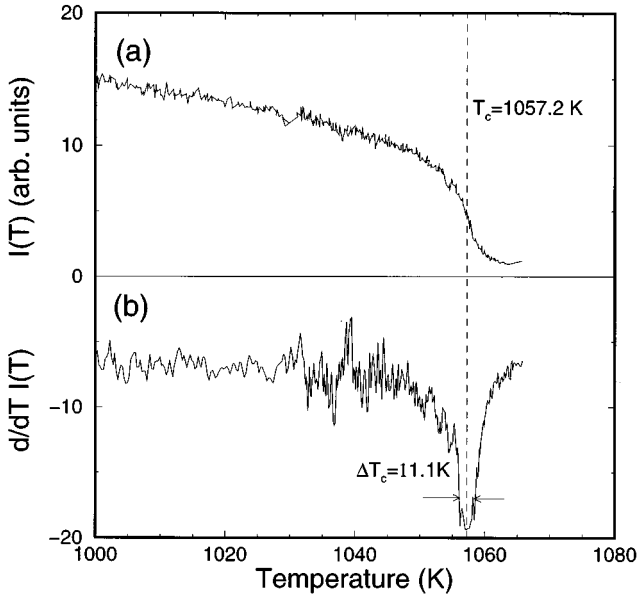

FIG. 3. Peak intensity of the $(\frac{1}{3}\frac{1}{3})$ spot versus temperature after Debye-Waller correction. The derivative of (a) with respect to temperature is shown in (b). The minimum in (b), i.e., the inflection point of the curve shown in (a), was used to estimate T_c.

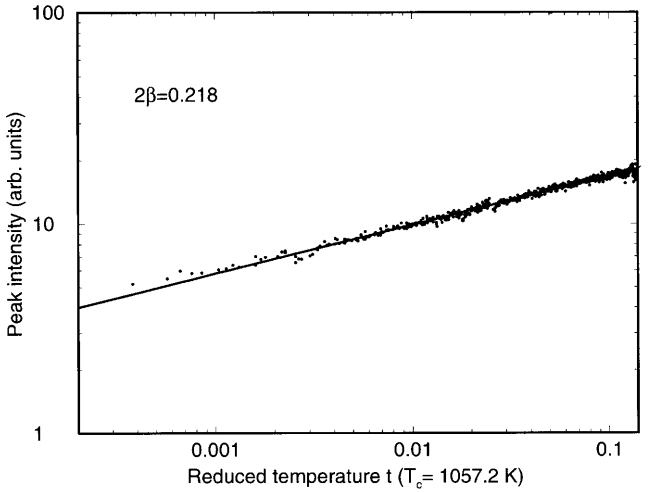

FIG. 4. Log-log plot of the peak intensity of a $(\frac{1}{3}\frac{1}{3})$ spot as a function of reduced temperature below T_c. The slope of the fitted power law yields an exponent $2\beta=0.218$ for this data set.

Above T_c, no intensity from long-range order exists, so that the critical scattering can be analyzed quantitatively. Since the measurements of critical scattering were done at roughly twice the bulk Debye temperature of Si ($1050<T<1120$ K), we had to subtract a relatively large background due to thermal diffuse scattering. Therefore, the background intensity and its temperature dependence were measured independently at a location as far away from the Bragg positions as possible, i.e., in our case $\frac{1}{6}(2\pi/a)$ away from the $(\frac{1}{3}\frac{1}{3})$ spot. Since this background turned out to depend little on $q_\parallel$ and on temperature, a parametrization of the temperature dependence was possible for background subtraction.

Figure 5 shows some typical high-resolution profiles of the $(\frac{1}{3}\frac{1}{3})$ spot at temperatures both above and below T_c. After subtracting the background, the data were fitted according to Eq. (2.1). The critical exponents ν and γ were determined

TABLE I. Summary of experimentally determined critical exponents and comparison with theoretical models. Good agreement with the three-state Potts model can be seen.

		Theory			
	Experiment	Ising	three-Potts	four-Potts	1st order
β	0.113 ± 0.005	0.125	0.111	0.0833	0
ν	0.87 ± 0.07	1	0.833	0.666	0.5
γ	1.35 ± 0.12	1.75	1.44	1.17	1

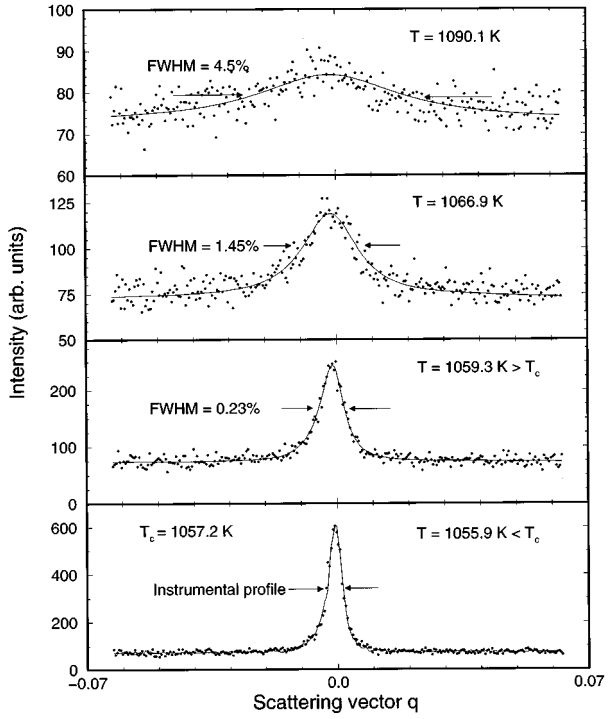

FIG. 5. Typical high-resolution profiles of the $(\frac{1}{3}\frac{1}{3})$ spot at temperatures below T_c (a) and above T_c (b)–(d). The scattering vector q parallel to the surface and the half widths (full width at half maximum) are given in units of k_{10}.

from plots of ξ and χ_0 versus reduced temperature (see Figs. 6 and 7). In order to make sure that T_c does not change, peak-intensity curves versus temperature such as Fig. 2 were measured routinely between the profile measurements.

Both ξ and χ_0 show scaling over the reduced temperature range $0.001<t<0.05$. The error bars shown have two main origins. At large reduced temperatures the error is dominated by the uncertainty in background subtraction, since the diffraction peaks were weak and broad. At the right-most data point ($t=0.06$) the signal to background ratio was as small as 1:10. At small reduced temperatures, on the other hand, the main source of error is the lack of precise knowledge of

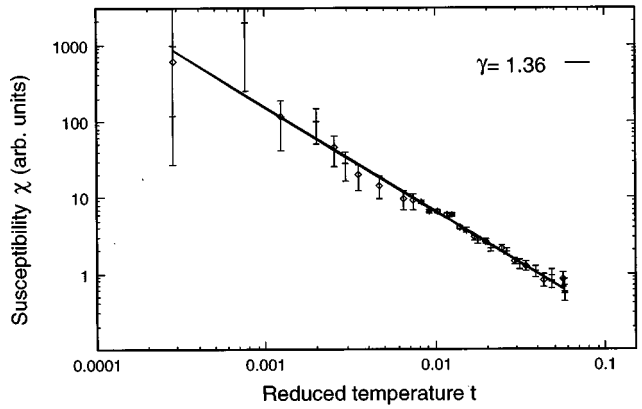

FIG. 6. Log-log plot of the amplitudes of critical scattering χ_0 versus reduced temperature above T_c. Slope yields exponent γ. Different symbols represent data sets taken in two orthogonal scan directions (for details, see text).

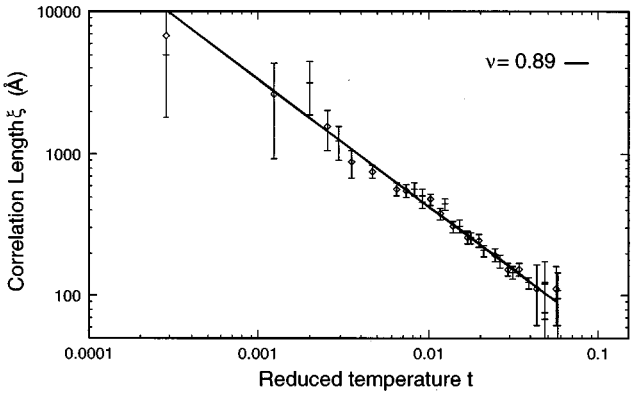

FIG. 7. Log-log plot of the correlation lengths ξ versus reduced temperature above T_c. Slope of fit yields exponent ν. Different symbols represent data sets taken in two orthogonal scan directions.

the instrument function. Small changes in the measured instrument function significantly affected the result of the fit. The temperature range at small t is also limited by temperature resolution and stabilization, as mentioned before. For the power-law fit, every data point was weighted inversely with its uncertainty. The analysis of radial and tangential cuts through the spot profiles yielded identical results. Therefore, the two orthogonal scan directions of the same diffraction spot were plotted and analyzed together.

No finite-size effects are visible, which would show up as a leveling off of correlation lengths and susceptibility values at small reduced temperatures. This indicates that we are not limited by the terrace widths or other kinds of frozen defects in this system. The precision in determining the critical exponents ν and γ depends mainly on the quality of the fit and on the uncertainty in T_c. The uncertainty for both critical exponents caused by ΔT_c is approximately 5%. Together with the variance of the fit we estimate an overall uncertainty of about 8%. Our results for the critical exponents ν and γ of correlation length and susceptibility are again summarized in Table I, where the average values of several independent data sets measured at both the $(\frac{1}{3}\frac{1}{3})$ and $(\frac{2}{3}\frac{2}{3})$ spots are shown. The critical exponents are in good agreement with those theoretically expected for the three-state Potts model.

IV. DISCUSSION

As our experiments show, all superstructure spots of the $\sqrt{3}\times\sqrt{3}$R30° phase exhibit the same temperature behavior. There is no indication for the appearance of another ordered structure. We take these observations as proof that this structure undergoes a true order-disorder phase transition. From symmetry arguments applied to a lattice gas,[4] a continuous order-disorder phase transition of a $\sqrt{3}\times\sqrt{3}$R30° phase is expected to belong to the three-state Potts universality class, in close agreement with our experimental results. We also would like to point out that only this quantitative agreement with the predicted universality class can be taken as evidence for a continuous phase transition, whereas the mere missing of hysteresis is not sufficient.[15]

The validity of this pure symmetry argument can be well demonstrated by the existing data for order-disorder phase transitions within this universality class. Previous quantita-

tive measurements of the critical properties of order-disorder transitions of $\sqrt{3}\times\sqrt{3}$R30° phases have been carried out, e.g., for $\sqrt{3}\times\sqrt{3}$R30°-S/Ru(0001) (Ref. 6) and for Kr/graphite.[39] Their ordered structures just contain one atom per unit cell, 1/3 ML coverage. What matters only, however, is the existence of three equivalent sublattices in the ordered structure, which have the same point symmetry as the disordered phase. Even the partial change of site associated with the phase transition found for the S/Ru(0001) system recently[40] does not seem to be relevant for the critical properties as long as there is a finite energetic difference between these adsorption sites, as tested by Monte Carlo simulations for this system.[41]

From our experiment we also conclude that the condition of free particle exchange between the $\sqrt{3}\times\sqrt{3}$R30° phase and the Au islands is obviously sufficient to make any coupling between the field conjugate to the order parameter and the chemical potential irrelevant, so that the unrenormalized critical exponents can be observed. This is in contrast to the condition of constant coverage of the ordered phase, which acts as a constraint, since in many cases the chemical potential also varies critically as a function of concentration. As a consequence, we get almost perfect agreement between theory and experiment for β, the critical exponent of the order parameter. Here also the largest range in t (two orders of magnitude) and the highest quality of data were available. The small contribution of critical scattering below T_c is in agreement with Monte Carlo simulations carried out earlier.[42] The larger deviations between experiment and theory for exponents ν and γ might mostly be due to the larger uncertainties in the experimental data for these two quantities, and to the smaller available range in t. The influence of corrections to scaling cannot be totally excluded, however, but curvatures of the log-log plots can only be detected over many orders of magnitude of t. Therefore, our determination is restricted to effective critical exponents.

Although the critical exponents are only sensitive to pure changes of symmetry, the question arises how the disordering proceeds in the system under investigation here. While no conclusive answer can be given based on the data presented here, the most likely and simplest possibility is the removal of trimerization, which involves both Au and Si atoms of the first substrate layer according to a structural model developed in Ref. 17. Although even this simple mechanism would cause local structural changes, compared to the ordered layer, these changes do not directly affect our data evaluation. The corresponding changes in LEED intensity only occurs in the integral order spots, since the superstructure spots measure only the $\sqrt{3}\times\sqrt{3}$R30°-correlated part of the layer, where no drastic changes of local geometry compared to the fully ordered layer should have occurred. In analogy to the results for S/Ru(0001), we conclude that even if there are changes of sites involved in the phase transition, we would get the same critical behavior as measured as long as there is a finite energetic difference between those sites.

As mentioned in the last section, our data analysis was not limited by finite-size effects up to the largest measured correlation lengths ($\approx$5000 Å), but mostly by finite instrument and temperature resolution. This fact is remarkable, because we measured in equilibrium with three-dimensional islands, which may act as frozen defects depending on their mobility. The lack of any influence of these islands on the critical properties is understandable from the SEM observations [Fig. 1(b)], which reveal that the islands preferentially nucleate at step bunches, but the terraces are scarcely covered by islands. Although single steps are not visible in Fig. 1(b), the average distance between steps is of the order of μm. Therefore, for correlation lengths up to a few thousand Å, which was the limit in our experiments, no influence by the presence of the islands should be expected. Because these islands are very sparce, they cannot be detected by diffraction.

Summarizing, we have shown that the Si(111)-$\sqrt{3}\times\sqrt{3}$-Au phase undergoes a true order-disorder continuous phase transition above 1000 K, as indicated by the determined critical exponents β, γ, and ν. The situation of thermodynamic equilibrium between 3D islands of excess Au atoms and the 2D $\sqrt{3}\times\sqrt{3}$R30° phase made the measurements possible without the constraint of constant coverage, a unique situation for chemisorbed adsorbates. Our results show that the quantitative evaluation of critical scattering is not limited to metal surfaces, although the reconstructions involved on semiconductor surfaces are usually much more complicated than on metals. Si(111) surfaces are in fact attractive for these measurements, since limitations in these experiments are only due to instrumental resolution, but not due to finite-size effects of the substrate surface.

ACKNOWLEDGMENTS

This work was done under a Monbusho International Scientific Research Program (No. 07044133) conducted by Professor Katsumichi Yagi of Tokyo Institute of Technology. We acknowledge Professors Shozo Ino of University of Tokyo and Martin Henzler of Hannover University for their valuable discussions and continuous support. Keinosuke Toriyama kindly helped us on operating SEM.

*Electronic address: pfnuer@dynamic.fkp.uni-hannover.de

[1] E. Bauer, in *Structure and Dynamics of Surfaces II*, edited by V. Schommers and P. von Blanckenhagen, *Topics in Current Physics* Vol. 43 (Springer, Berlin, 1987), p. 115.

[2] K. Binder and D. Landau, in *Molecule-Surface Interaction*, edited by K. Lawley (Wiley, New York, 1989), p. 91.

[3] B. N. J. Persson, Surf. Sci. Rep. **15**, 1 (1992).

[4] M. Schick, Prog. Surf. Sci. **11**, 245 (1981).

[5] H. Pfnür and P. Piercy, Phys. Rev. B **40**, 2515 (1989).

[6] M. Sokolowski and H. Pfnür, Phys. Rev. B **49**, 7716 (1994).

[7] D. Matthews-Morgan, D. P. Landau, and H. Swendsen, Phys. Rev. Lett. **53**, 679 (1984).

[8] M. Novotny and D. Landau, Phys. Rev. B **32**, 3112 (1985).

[9] S. Chen, A. M. Ferrenberg, and D. P. Landau, Phys. Rev. Lett. **69**, 1213 (1992).

[10] C. Voges, K. Budde, and H. Pfnür, Surf. Sci. **338**, L839 (1995).

[11] K. Budde, L. Schwenger, C. Voges, and H. Pfnür, Phys. Rev. B **52**, 9275 (1995).

[12] M. Sokolowski, M. Lindroos, and H. Pfnür, Surf. Sci. **278**, 87 (1992).

[13] M. Sokolowski and H. Pfnür, Phys. Rev. Lett. **63**, 183 (1989).
[14] S. Ino, in *Reflection High Energy Electron Diffraction and Reflection Electron Imaging of Surfaces*, edited by P. K. Larsen and P. J. Dobson (Plenum, New York, 1988).
[15] S. Hasegawa, Y. Nagai, T. Oonishi, and S. Ino, Phys. Rev. B **47**, 9903 (1993).
[16] S. Hasegawa, Y. Nagai, T. Oonishi, N. Kobayashi, T. Miyake, S. Murakami, Y. Ishii, D. Hanawa, and S. Ino, Phase Transit. **53**, 87 (1995).
[17] Y. G. Ding, C. T. Chan, and K. M. Ho, Surf. Sci. **275**, L691 (1992).
[18] K. Higashiyama, S. Kono, and T. Sagawa, Jpn. J. Appl. Phys. **25**, L117, (1986).
[19] J. Quinn, F. Jona, and P. M. Marcus, Phys. Rev. B **46**, 7288 (1992).
[20] M. Ichikawa, T. Doi, and K. Hayakawa, Surf. Sci. **159**, 133 (1985).
[21] S. Takahashi, Y. Tanishiro, and K. Takayanagi, Surf. Sci. **242**, 73 (1991).
[22] R. Plass and L. D. Marks, Surf. Sci. **342**, 233 (1995).
[23] K. Oura, M. Katayama, F. Shoji, and T. Hanawa, Phys. Rev. Lett. **55**, 1486 (1985).
[24] J. H. Huang and R. S. Williams, Phys. Rev. B **38**, 4022 (1988).
[25] R. S. Daley, J. Huang, and R. S. Williams, Surf. Sci. **202**, L577 (1988).
[26] M. Chester and T. Gustafsson, Phys. Rev. B **42**, 9233 (1990).
[27] M. Chester and T. Gustafsson, Surf. Sci. **256**, 135 (1991).
[28] D. Dornisch *et al.*, Phys. Rev. B **44**, 11 221 (1991).
[29] Y. Kuwahara, S. Nakatani, M. Takahasi, M. Aono, and T. Takahashi, Surf. Sci. **310**, 226 (1994).
[30] J. Nogami, A. A. Baski, and C. F. Quate, Phys. Rev. Lett. **65**, 1611 (1990).
[31] J. Nogami, K. Wan, and J. C. Glueckstein, Jpn. J. Appl. Phys. **33**, 3679 (1994).
[32] T. Takami, D. Fukushi, T. Nakayama, M. Uda, and M. Aono, Jpn. J. Appl. Phys. **33**, 3688 (1994).
[33] J. Falta *et al.*, Surf. Sci. **330**, L673 (1995).
[34] T. Nagao and S. Hasegawa (unpublished).
[35] U. Scheithauer, G. Meyer, and M. Henzler, Surf. Sci. **178**, 441 (1986).
[36] T. Tsuno, Ph.D. thesis, University of Tokyo, 1990.
[37] H. E. Stanley, *Introduction to Phase Transitions and Critical Phenomena* (Oxford University Press, New York, 1971).
[38] N. C. Bartelt, T. L. Einstein, and L. Roelofs, Phys. Rev. B **32**, 2993 (1985).
[39] P. M. Horn, R. J. Birgeneau, P. Heiney, and E. M. Hammonds, Phys. Rev. Lett. **41**, 961 (1978).
[40] C. Schwennicke, C. Voges, and H. Pfnür, Surf. Sci. **349**, 185 (1996).
[41] C. Schwennicke, and H. Pfnür (unpublished).
[42] N. Bartelt, T. Einstein, and L. Roelofs, Phys. Rev. B **35**, 6786 (1987).